

The Discretised Population Model of Turbulence

Figure Showing Three Chemical Reaction Regions (see page 12)

PHOENICS-2017

PHOENICS-2017-V1 Release: Mid April

PHOENICS-2017 will be released mid April 2017. As well as bug fixes and small enhancements to Core and FLAIR, the major items features in this version are:

- High-Re Realisable k-e model
- Improved k- ω model
- Scalable wall functions
- Improved Fine-Grid-Volume (FGV) (*speed/parallel operation to follow.*)
- Lawson criteria for wind comfort (FLAIR)
- Improved rain model (FLAIR)
- Air Exchange Effectiveness for individual rooms (FLAIR)
- Age of air for individual rooms (FLAIR)
- Inclusion of Belgian / Dutch / FRS fire models (FLAIR)

PHOENICS-2017-V1 Release: July

Items in-progress for inclusion in next release of PHOENICS-2017 include:

- Revised Wilcox k- ω model
- Menter-Wilcox k- ω model
- k- ω SST model
- DES (Detached Eddy Simulation), a variant of LES
- DFM for particle deposition & transport (FLAIR)
- Continued improvement of FGV
- Inclusion of CHAM-J free-surface model (THINC VOF with surface tension and contact angle)
- Revision of PARSOL (X-PARSOL)
- IPSA model improvements for modelling dense solid media (e.g. blast furnace, avalanche)

Ongoing Development Items

Additional development resources have been allocated. The following tasks are being undertaken in parallel with the above items:

- Update F1 VWT Simscene to latest release of PHOENICS Direct
- Finalise Heatex Simscene with updated PHOENICS Direct
- Implementation of two-phase Volume Of Fluid (CISIT VOF with mass transfer) model
- Acceleration of parallel solver
- Inclusion of replacement multi-grid and coupled solvers
- Re-evaluation of Unstructured PHOENICS

The current release version of PHOENICS (dated October 2016) is described at: www.cham.co.uk/phoenics/d_polis/d_docs/tr006/tr006.pdf

Damping of wind induced vibration in tall buildings

Dr R. P. Hornby e-mail: bob@hornby007.wanadoo.co.uk

Introduction

On August 4th 2016, after two years of construction, the Brighton i360 Tower opened. It was created by the same team that constructed the London Eye. It stands on a site once occupied by the entrance to Brighton's ruined west pier (figure 1) and is 162m high with a slenderness ratio of 1:40 (the Shard is 1:6). It is both the World's thinnest tower with a 4.5m diameter and the World's tallest moving observation tower. An important design aspect for such a tall structure is its ability to withstand high winds and storms without vibration causing discomfort for people in the observation pod (which is entered at ground level and moves up to the top of the tower).

The vibration is caused by wind buffeting and vortex shedding around the structure. In the case of vortex shedding, the shedding frequency f (Hz) can be obtained from the Strouhal Number, S

$$S = \frac{fD}{V}$$

where $D(m)$ is the structure diameter and $V(ms^{-1})$ the wind speed. The Reynolds Number based on tower diameter will be of order 10^{---7} suggesting a value of S of about 0.3. This would give a vortex shedding frequency close to 1Hz for a wind speed of $15ms^{-1}$.

There are various ways of damping such vibrations but increasing use is being made of Tuned Sloshing Water Dampers (TSWDs). TSWD is essentially a tank rigidly attached to the structure, the sloshing frequency of the water in the tank tuned with the structure's prime vibrational frequency. The sloshing causes dissipation of some of the energy imparted to the structure causing a reduction in the amplitude of vibration.

For a rectangular tank the first (prime) sloshing frequency, f , is given by (Ref 1).

$$f = \frac{1}{2\pi} \sqrt{\left(\frac{3.16g \tanh\left(3.16 \frac{h}{L}\right)}{L} \right)}$$

where $g(ms^{-2})$ is the acceleration due to gravity, $h(m)$ the water depth and $L(m)$ the box dimension in the direction of sloshing.

For example, a rectangular box with a sloshing length of 0.5m and water depth of 0.2m would have a prime sloshing frequency of 0.94Hz.



Figure 1. The 162m high Brighton Tower showing the observation pod at height.



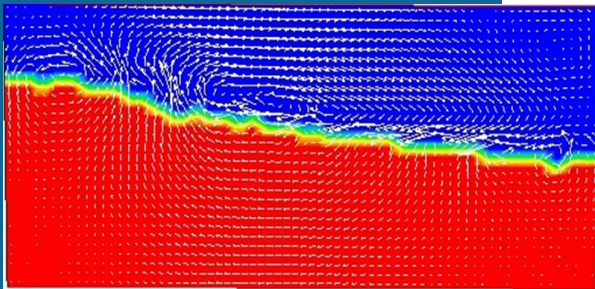
Figure 2. An array of MTSWDs being prepared for use in the Brighton Tower. Note the different box depth.



This shows that relatively small box dimensions can achieve the low structural modal frequencies required and match specific tower vortex shedding frequencies. By changing box size or water depth, a range of frequencies can be catered for. These systems are termed Multiple frequency Tuned Slushing Water Dampers (MTWSDs), and are applicable to structures with multiple modes of vibration (figure 2 page 3).

The Brighton Tower design seeks to minimize the effects of vortex shedding by using a roughened aluminium cladding on its surface. The cladding is perforated to allow the wind to flow through it, so disrupting the regular formation of vortices. MTSWDs are also fitted inside the tower (in the pod and at 3 different levels, though with the majority at the tower top) to further reduce vibration. The dimensions of the dampers are calculated so that they tune to the frequencies of the first 3 modes of vibration of the tower.

Figure 3. A typical PHOENICS slushing profile (the red colour tags water; the blue colour, air). The tank size is 0.285m by 0.285m by 0.120m high with a static water depth of 0.08m. The forcing frequency is 1.628Hz.



PHOENICS modelling and results

The Scalar Equation Method (SEM, including the correction outlined in Ref 2) is used to model the fluid slushing in a rectangular tank. A 2-D transient analysis is carried out using a uniform mesh in the y (slushing) and z (vertical) directions. Laminar flow is assumed and surfaces are assumed frictionless. A typical result from one of the PHOENICS runs is shown in figure 3.

Ref 3 gives experimental results for a square tank of side 0.270m and 0.3m height. This is filled with water to a depth of 0.15m and subjected to a fixed amplitude sinusoidal excitation at a given frequency. The amplitude of the slushing motion is measured over a range of frequencies and the frequency producing the largest amplitude is taken as the prime slushing frequency. PHOENICS results for this case are shown in figure 4 for runs with 50 by 50 and 100 by 100 cells showing good agreement with experimental value of 1.63Hz.

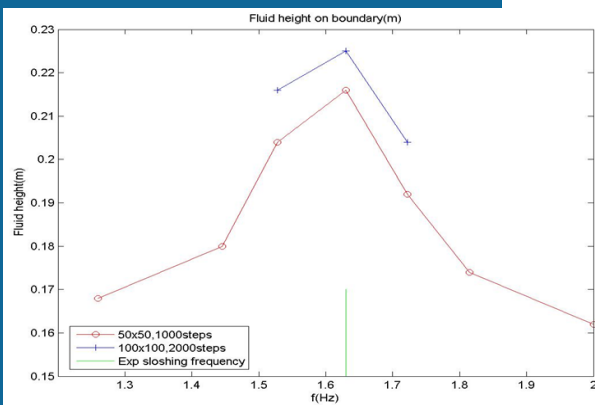


Figure 4. Results for a square tank of side 0.270m and 0.3m height filled with water to a depth of 0.15m. The plot shows the maximum fluid height on the tank wall as a function of forcing frequency (the forcing amplitude is kept constant).

Net force (applied force minus slushing force) acting on the TSWD was not significantly reduced in those PHOENICS runs without any resistance to the slushing flow (i.e. runs without wall friction or screens or orifices etc placed in the tank).

However, a large reduction in the net force was produced when a phase shift close to 180° between the applied force and the response force resulted from including resistive effects into the tank.

To illustrate this, results are presented for a square tank of side 0.285m and 0.120m height filled with water to a depth of 0.08m. Dimensions and water depth are those of 44 of the 1649 MTSWDs proposed for retrofitting an existing four storey building with a total slushing water mass of 6638kg (Ref 4).



Dimensions and water depth are those of 44 of the 1649 MTSWDs proposed for retrofitting an existing four storey building with a total sloshing water mass of 6638kg (Ref 4).

In the PHOENICS model the forcing is achieved by a sinusoidal source term per unit volume of water introduced into the y direction momentum equation. Resistive effects are modelled as a $-y$ direction force per unit volume of water proportional to the local water y direction velocity. This is a relatively simple way of illustrating the main features of a resisted flow, though in a practical case detailed modelling of screens, flow orifices or other flow resistive components would be required and can be fully accommodated by PHOENICS.

The results for a forcing frequency of 1.48Hz and resistance factor of 15 are shown in figure 5. In particular the resistive component introduces a phase shift in response relative to applied force so that the net force is significantly reduced. This is illustrated in figure 6. Mean power is defined as the sum of the amplitudes squared divided by the fixed simulation time. The results compare the mean power in each signal (net force and applied force) as a function of forcing frequency for a fixed resistance factor. This shows that a maximum reduction in mean power in excess of 80% occurs at a frequency of 1.7Hz.

These results indicate the scope available with this type of analysis to optimise the performance of TSWDs at specified frequencies.

Conclusions

The PHOENICS SEM has been used to model the sloshing of water in a TSWD. Good agreement with experiment has been obtained for the fundamental sloshing frequency in a rectangular tank and some simple modelling has shown how effective a TSWD can be in reducing the amplitude of forced structural vibrations. A more extensive study could help optimize use of particular resistive components in the TSWD.

References

1. Housner G. W. Dynamic analysis of fluids in containers subjected to acceleration. Nuclear Reactors and Earthquakes, Report No. TID7024, U.S. Atomic Energy Commission, Washington D.C., 1963.
2. PHOENICS Newsletter, Spring 2016.
3. Jaiswal O. R., Shraddha Kulkarni and Pavan Pathak. A study of sloshing frequencies of fluid-tank system. 14th World Conference on Earthquake Engineering, Beijing, China, October 2008.
4. Nishant Kishore Rai, Reddy G. R. and Venkatraj V. Tuned liquid sloshing water damper: a robust device for seismic retrofitting. International Journal of Environmental Science: Development & Monitoring (IJESDM) ISSN No. 2231-1289, Vol 4 No. 2, 2013.

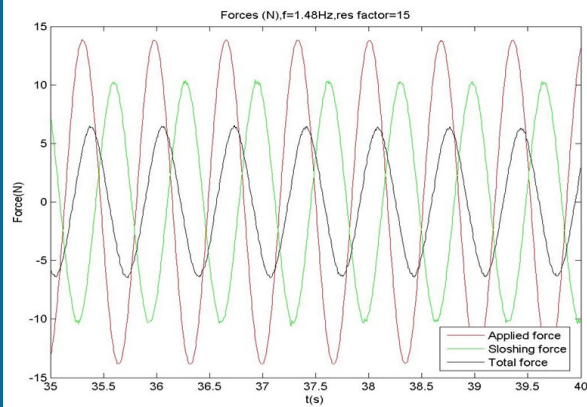


Figure 5. Results for sloshing in a square box of side 0.285m and height 0.120m filled with water to a depth of 0.80m. Forcing frequency is 1.48Hz and the resistance factor is equal to 15. Note the phase shift between the applied force and the sloshing force.

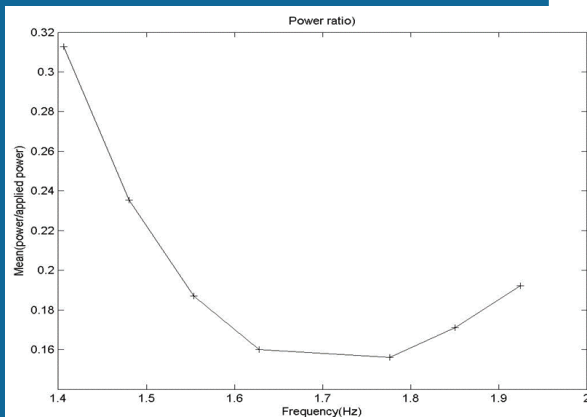


Figure 6. Results for sloshing in a square box of side 0.285m and height 0.120m filled with water to a depth of 0.80m for a range of forcing frequencies at a fixed resistance factor of 15.

Using CFD in the Analysis of Thermal Sterilisation of Liquid Foods

Abdul Ghani Albaali, PHOENICS Software User, Princess Sumaya University for Technology, Amman-Jordan , (Previously University of Auckland, Auckland-New Zealand)

Abstract

Sterilisation of liquid food in cans and pouches was studied and analysed using computational fluid dynamics (CFD). The software package code PHOENICS was used, which is based on finite volume method of analysis (FVM). The results of the simulations were presented in the form of transient temperature, velocity profiles and flow patterns, live bacteria and vitamin concentrations. The shapes and movement of the slowest heating zone were followed throughout the sterilisation time.

1) Simulation of Sterilisation of food in a vertical can

In this part of the work, sterilisation of canned liquid food in a metal can sitting in an upright position and heated by steam at 121°C from all sides was studied. A solution of sodium carboxy methyl cellulose (CMC) was used as a model liquid. The objective of this work was to study the effect of the natural convection current on the movement of the slowest heating zone (SHZ) during sterilisation. The computations were performed for a two-dimensional can with a radius of 40.5 mm and a height of 111 mm. A non-uniform grid system was used in the simulations with 3519 cells: 69 in the axial direction and 51 in the radial direction, graded in both directions with a finer grid near the wall. The natural convection heating of CMC was simulated for 2574 s. The partial differential equations governing natural convection motion in a cylindrical space are the Navier-Stokes equations in cylindrical coordinates

Figure 1 show, the temperature profile, velocity vector and the flow pattern of the CMC in a can heated by steam condensing along its outside surface. Figure 1 (a) shows the influence of natural convection current on the movement of the SHZ in the can (i.e. the location of the lowest temperature at a given time). Both Figures 1 (b) and 1 (c) show a re-circulating flow created by the buoyancy force, which is due to temperature variation (from the wall to the core). A secondary flow is also observed at the bottom of the can, which influence the heat transfer within the

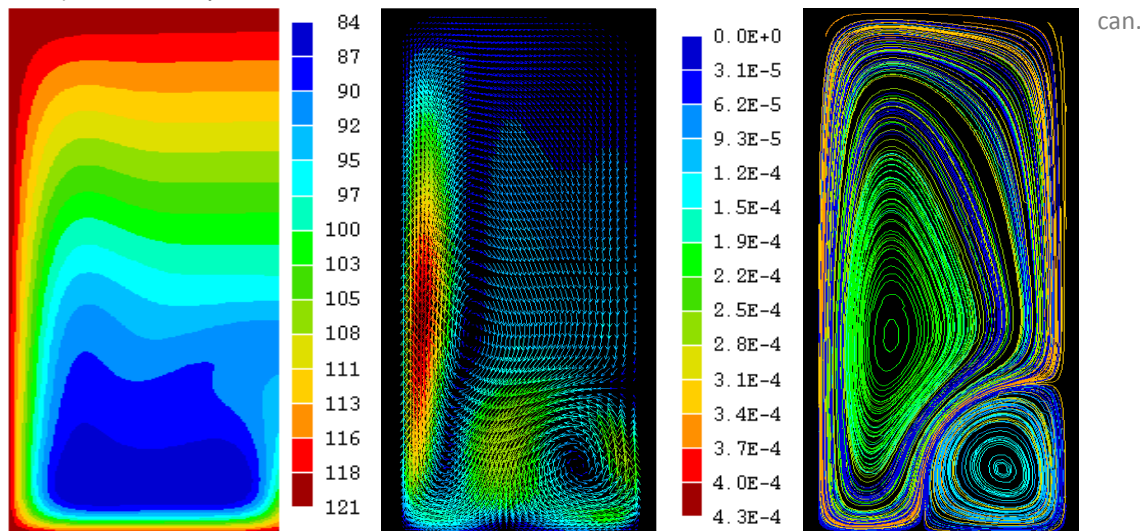


Figure 1: Temperature profile, Velocity vector and flow pattern of CMC in a vertical can after 1157 s heat treatment by condensing steam. The right-hand side of each figure is centreline.

2) Simulation of bacteria deactivation during sterilisation

The objective here is to obtain improved quantitative understanding of the effect of natural convection heating upon bacterial deactivation during thermal sterilisation. In this simulation, a computational procedure is also developed for describing the changes in live bacteria concentration and its transient spatial distributions during sterilisation processing of canned food. The model parameters are the same as those used in the previous simulation. The governing equations of continuity, momentum and energy are solved together with that of live bacteria concentration.

Mass Balance for bacteria:

$$\frac{\partial C_{rb}}{\partial t} + v \frac{\partial C_{rb}}{\partial r} + u \frac{\partial C_{rb}}{\partial z} = D \left[\frac{1}{r} \frac{\partial}{\partial r} \left(r \frac{\partial C_{rb}}{\partial r} \right) + \frac{\partial^2 C_{rb}}{\partial z^2} \right] - k_T C_{rb}$$



Where C_{rb} = relative bacteria concentration (C_b/C_{bo}); D = diffusion coefficient of bacteria, $m^2 s^{-1}$; t = exposure time, s; k_T = reaction rate constant of bacteria deactivation, s^{-1} ; u, v = velocity in vertical and radial direction, ms^{-1} ; r = radial position from centre line, m; z = distance in vertical direction from the bottom, m.

Arrhenius equation is used to describe the kinetics of bacterial death and the influence of temperature on the reaction rate constant. It is introduced to the software package using FORTRAN code. Figure 2 shows the results of the simulation for the same metal can filled with CMC, steam heated from all sides (at $121^\circ C$). Figure 2 (a) shows that during the early stage of heating, the bacteria are killed only at locations close to the wall of the can, and are not influenced by the flow induced by natural convection. Figures 2 (b) and 2 (c) show the results of the simulation after much longer time of 1157 s and 2574 s respectively.

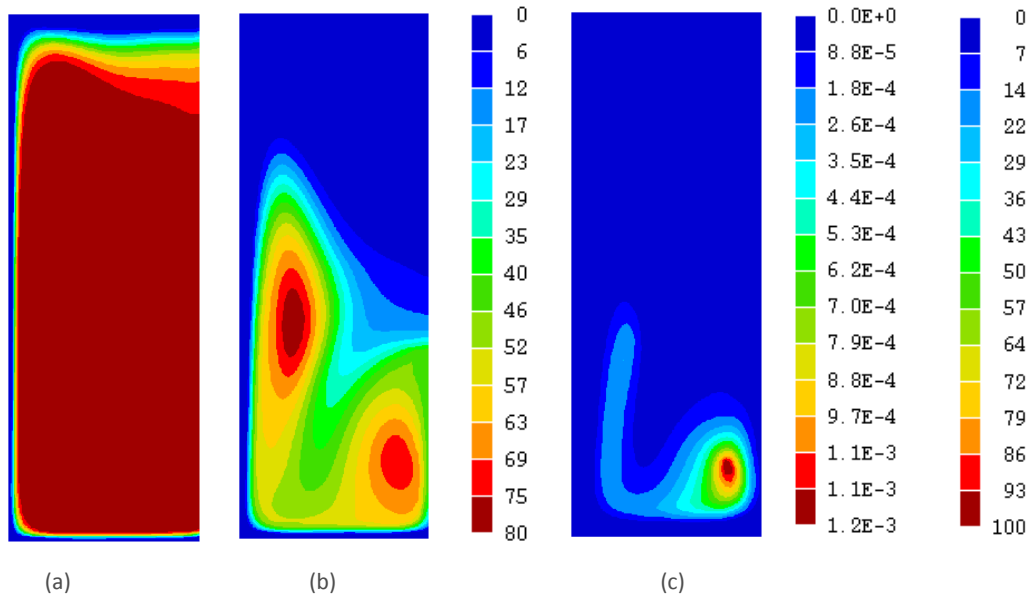


Figure 2: Deactivation of bacteria in a can filled with CMC and heated by condensing steam after (a) 180 s, (b) 1157 s and (c) 2574 s. The right-hand side of each figure is centreline.

3) Simulation of Vitamins destruction during sterilisation

Profiles of concentrations of Vitamin C (ascorbic acid), B1 (thiamin) and B2 (riboflavin) in a can filled with viscous liquid food (concentrated cherry juice) during thermal sterilisation were presented and studied. The numerical model and the kinetics of the vitamins C, B1 and B2 destruction were similar to those for bacteria deactivation described in the previous section. The simulation highlights the dependency of the concentration of vitamins on both temperature distribution and flow pattern as sterilisation proceeds (Figure 3).

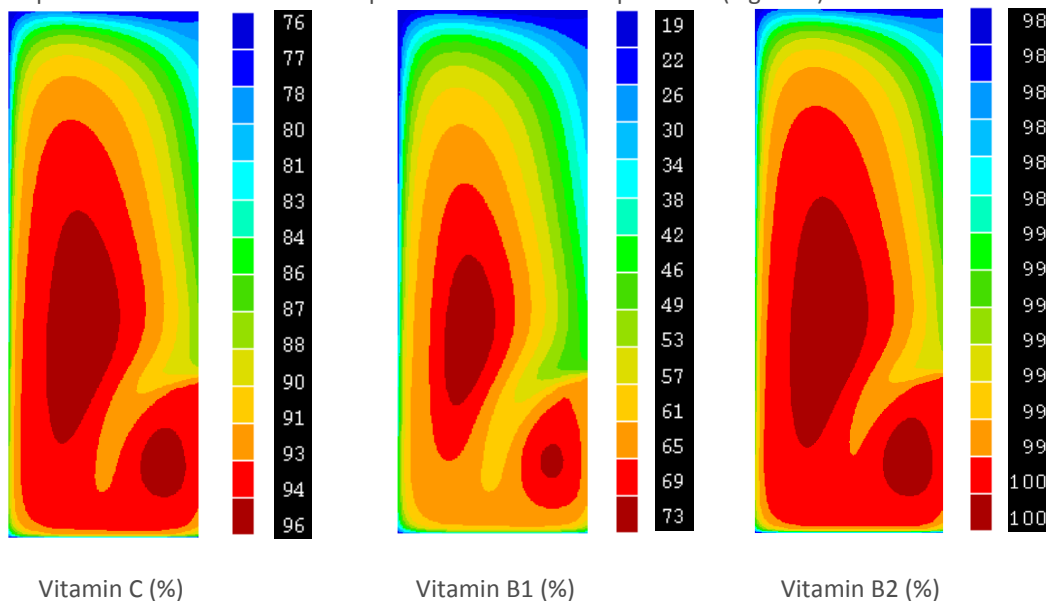


Figure 3: Destruction of vitamins in a can filled with concentrated cherry juice after 1640 s heat treatment by condensing steam. The right-hand side of each figure is centreline.



4) Simulation of a horizontal can during sterilisation

In this section, sterilisation of a canned liquid food in a metal can lying horizontally and heated at 121°C from all sides was predicted and studied. In the horizontal can, the axi-symmetry is not valid and the numerical solution has to be based on three dimensional analyses. A non-uniform grid system was used in the simulation with 105000 cells: 50 in the radial direction, 70 in the vertical direction and 30 in the angular direction, graded with a finer grid near the wall in radial and vertical directions. The natural convection heating of carrot-orange soup was simulated for 3000s. Figure 4, shows the radial-angular temperature profile of carrot-orange soup in a 3-D cylindrical can lying horizontally and heated by condensing steam after 600 s.

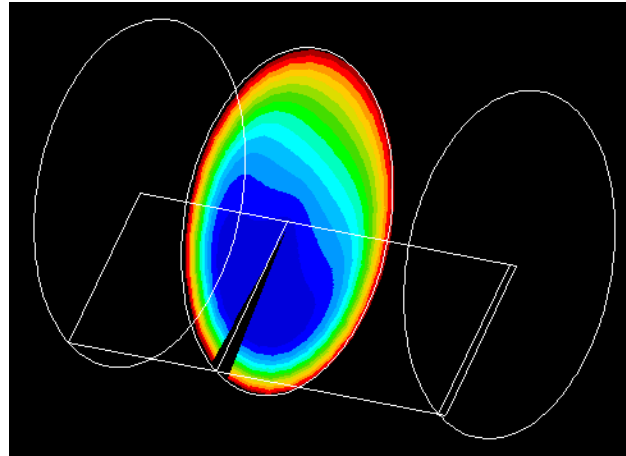


Figure 4: Radial-angular plane temperature profile of carrot-orange soup in a 3-D cylindrical can lying horizontally after 600 s heat treatment by condensing steam.

5) Simulation of sterilization of canned food in a 3-D pouch

In this study, transient temperature, bacteria deactivation, vitamin's destruction and the shape of the SHZ were presented for a uniformly heated three-dimensional pouch. The computations were performed for a 3-D pouch with a width of 120 mm, height of 35 mm and length of 220 mm. The pouch used in the simulations was divided into 6000 cells: 20 in the x-direction, 10 in the y-direction and 30 in the z-direction as shown in Figure 5.

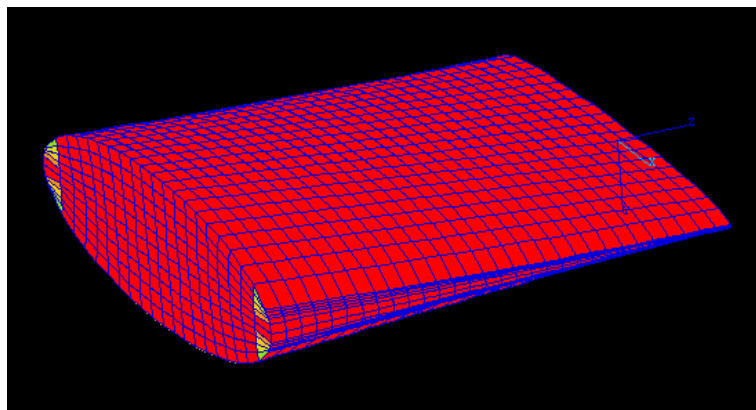


Figure 5: Pouch geometry and grid mesh

The heating was simulated for 3000s, the partial differential equations governing natural convection motion in a pouch space are the Navier-Stokes equations in x, y and z coordinates. The numerical procedure and the kinetics of bacteria deactivation and vitamins destruction were the same as those explained earlier. Figure 6 shows the temperature distribution at different y-planes in a pouch filled with carrot-orange soup at the end of heating (50min). This Figure shows the settlement of the SHZ at about 30% of the pouch height.

The heating was simulated for 3000s, the partial differential equations governing natural convection motion in a pouch space are the Navier-Stokes equations in x, y and z coordinates. The numerical procedure and the kinetics of bacteria deactivation and vitamins destruction were the same as those explained earlier. Figure 6 shows the temperature distribution at different y-planes in a pouch filled with carrot-orange soup at the end of heating (50min). This Figure shows the settlement of the SHZ at about 30% of the pouch height.

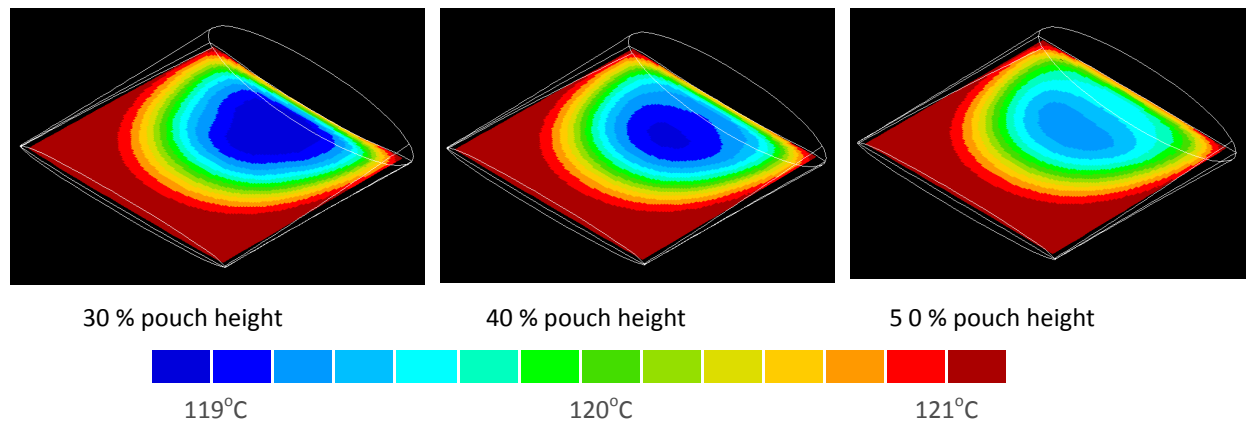


Figure 6: Temperature contours at different y-planes in a pouch filled with carrot-orange soup after 50 min heat treatment by condensing steam.

Figure 7 shows the relative concentration profiles of Vitamins C and B1 in the x-plane of the centre of the pouch. This figure shows the locations of a high vitamin concentration zone (HVCZ) at the two stagnant zones, which can be explained clearly in terms of x-plane velocity vector observed at the same axis and at the same time step.

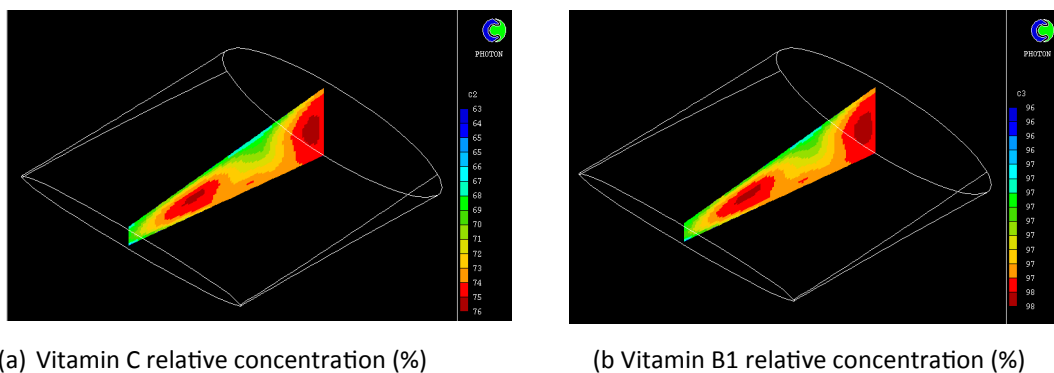


Figure 7: Relative concentration profiles of Vitamins C and B1 at 50% of x-plane of pouch filled with carrot-orange soup after 3000 s heat treatment by condensing steam.

Figure 8 shows the relative bacterial concentration profiles of *Clostridium botulinum*, for a pouch filled with carrot-orange soup and heated by condensing steam. The highest concentration of bacteria shown in Figure 8 occurs at two locations. These locations belong to minimum liquid velocity and low temperature zones.

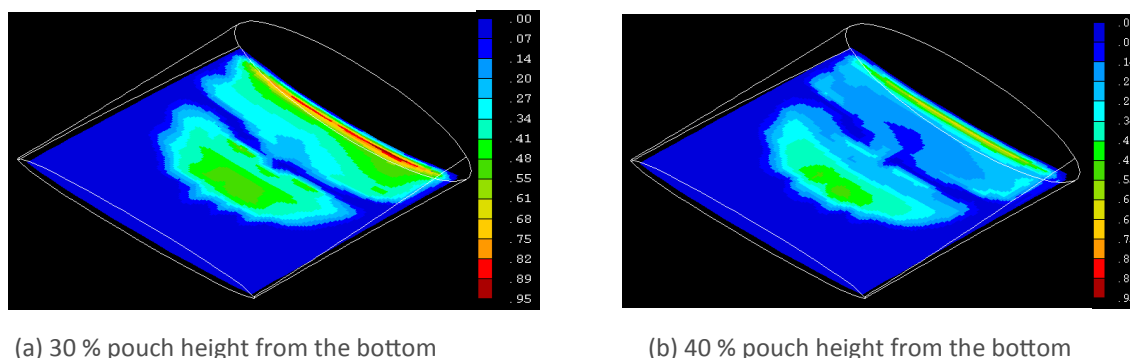


Figure 8: Relative concentration profiles of *Clostridium botulinum* at different y-planes in a pouch filled with carrot-orange soup after 1000 s heat treatment by condensing.



RhinoCFD: CAD to CFD powered by PHOENICS

RhinoCFD: The Integration of Two Worlds

CHAM is pleased to announce the commercial release of RhinoCFD, a new, unique, fully-integrated CAD to CFD user environment for Rhino3D powered by PHOENICS. RhinoCFD has been streamlined for easier intuitive and more efficient use, through simple and focused menu systems, allowing non-CFD users and CFD experts alike to perform state-of-the-art CFD simulations thus making a complex subject matter accessible to many new users. It also offers a wide range of result visualisation options allowing users both to inspect and present results easily.

It adds the power of computational fluid dynamics (CFD) to the CAD environment, allowing Rhino3D users to undertake interactive CFD investigations of their CAD models operating under a multitude of flow conditions. This facilitates rapid optimization and testing without leaving the familiar Rhino environment thus reducing the learning curve necessary to perform investigations.

What is CFD?

CFD helps predict and visualize how a fluid (gas or liquid) behaves and how it affects and interacts with objects that it encounters as it flows past. It enables users to test their models in real-world conditions without the cost of physically modelling them, saving valuable project testing time, optimizing their performance and reducing costs, leading to a more efficient project workflow.

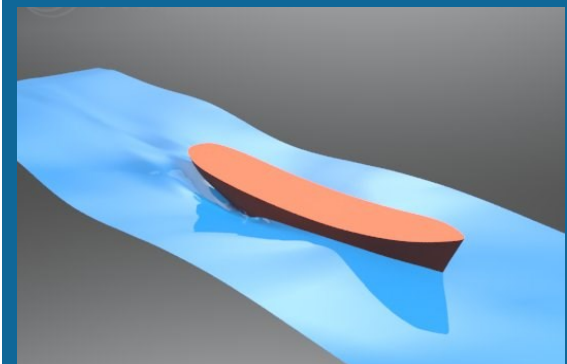
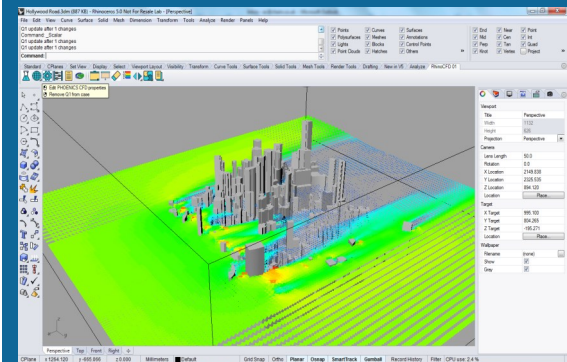
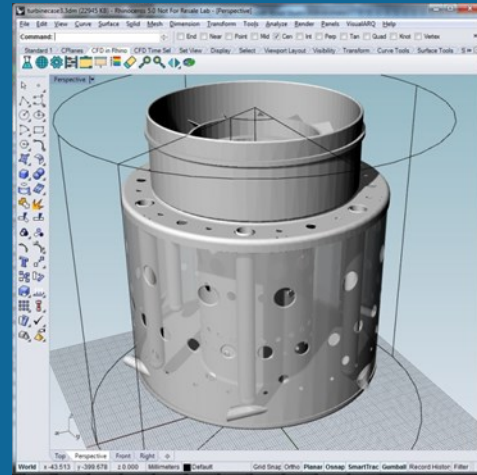
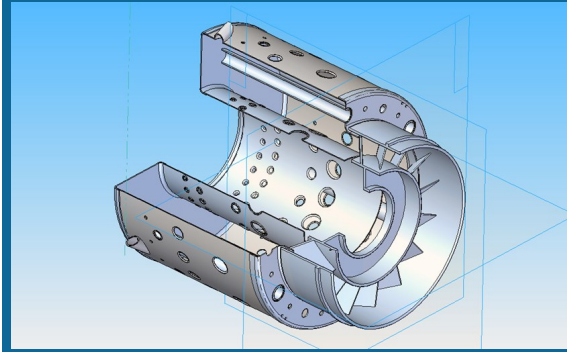
What are the benefits of RhinoCFD?

RhinoCFD provides a valuable aid to rapid prototyping, enabling designers and operators to:

- Save time by working in a familiar environment;
- Refine geometry and restart simulations as needed;
- Study flows in and around their CAD designs;.
- Test the consequential effects of design changes;
- Investigate, safely, "What if" scenarios; and
- Exemplify their operational parameters.

RhinoCFD incorporates many of the best and unique features of its mainstream PHOENICS counterpart:

- 'PARSOL' minimises problems associated with handling complex geometries.
- Automatic Meshing (structures Cartesian and Polar or Unstructured) avoids the necessity to spend hours optimizing meshes,
- CONWIZ, the convergence wizard, greatly reduces the complexity of obtaining converged solutions.
- Parallel Processing
- Free Surface modelling and Radiation modelling
- Standard and advanced turbulence-model options.



Both steady-state and transient (time-dependent) scenarios can be considered, enabling users to extend the range of conditions applied to their models.

RhinoCFD's scope allows simulation of complex phenomena such as multiple-phase and compressible flow, heat transfer both inside solids and between solids and fluids, radiation modelling and non-Newtonian flows.

Applications

CFD can be used in any area where fluids impact on a design. Its applications are numerous and it is used in a wide variety of industries including:

- Marine: design of hulls, sails, propellers
- Aerospace: Aerodynamics, turbomachinery, heat management
- Medical: Arterial flow, respiratory flow, effects of non-Newtonian fluids
- Jewellery: Investment casting optimization
- Architecture and building services: External/internal ventilation, HVAC, contaminant dispersion
- Transportation: Drag reduction, combustion processes, emissions testing

Commercial Release

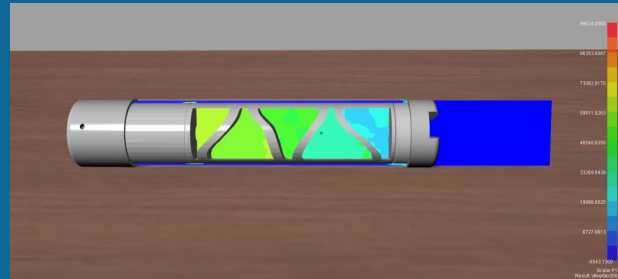
On March 15 SimplyRhino hosted a RhinoCFD workshop, in conjunction with CHAM, at the Goldsmiths Centre . CHAM's Engineering Manager, Andrew Carmichael, supported by Dr David Glynn and Dr Geoff Michel, from CHAM presented the product to 20 participants from industries including architecture, building services, consultancy and marine design. The event was aimed at providing both an introduction to CFD and basic concepts and a hands-on session with RhinoCFD to allow those present to explore how the program could be applied to their own particular projects.

Commercial Release

To celebrate the commercial release of RhinoCFD CHAM is offering a 30% discount to commercial users for purchases made in April.

Students and Academics may claim a 3 month free trial upon proof of status.

For more information, or to obtain RhinoCFD please contact SimplyRhino (info@simplyrhino.co.uk) which CHAM is pleased to announce is the first external distributor of RhinoCFD.



Integrated fluid flow simulation for Rhino3D

Choose RhinoCFD for a fully-integrated CAD to CFD user environment for Rhino3D.

To celebrate the commercial release of RhinoCFD CHAM is offering a 30% discount to commercial users for purchases in March and April. Students and Academics may claim a 3-month free trial on proof of status.



Participants at the Simply Rhino Workshop, March 15 2017



News from CHAM and its Agents

CHAM

PHOENICS-2017

CHAM is pleased to announce that PHOENICS-2017 V1 will be available from mid April (see page 2)

RhinoCFD Powered by PHOENICS

CHAM is also pleased to announce the commercial release of RhinoCFD, a new, unique, fully-integrated CAD to CFD user environment for Rhino3D powered by PHOENICS (see page 10).

PHOENICS Newsletter Contributions

CHAM would like to encourage all PHOENICS Users reading this Newsletter to contribute to it. Send articles to news@cham.co.uk, in Word format please. Academic Users please send your annual reports to the above email address for publication. Thank You.

Front Cover

The figure the cover comes from the paper associated with a lecture Professor Spalding gave on *The Discretised Population Model* in Sicily in September.

It was an extension of his earlier works relating to what was, then, called the Multi-Fluid Model. In the paper, Professor Spalding sought to describe “an entirely different type of turbulence model; which concentrates on sources rather than fluxes; and therefore can simulate practically-important phenomena about which all popular turbulence models must necessarily remain silent.” The model “can handle sources of all kinds, e.g. body-force, radiative, biochemical; but it is exemplified [in the paper] by reference to sources associated with chemical reaction.”

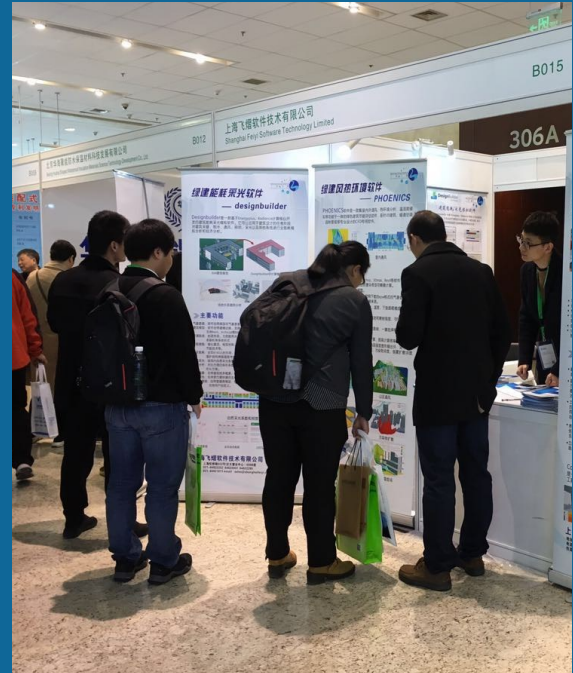
If you would like further information please contact news@cham.co.uk.

Shanghai Feiyi

Shanghai Feiyi participated in in the Thirteenth International Conference on Green and Energy-Efficient Building & New Technologies and Products Expo 21--22 March 2017.

SSC

Dr Alexey Ginevsky, of SSC in Moscow, will give a course of lectures in April to MSc Students. The course presents the basic concept of CFD and its application to heat exchangers and other topics of interest. PHOENICS forms the numerical basis of the lectures; the Students use the Software as the working numerical package from which they learn about general CFD features.



Shanghai Feiyi's stand at the Green and Energy – Efficient Building & New Technologies & Products Expo

Contents	Pg
PHOENICS-2017 Pre-Release Information	2
Damping of Wind Induced Vibration in Tall Buildings	3
Using CFD in the Analysis of Thermal Sterilisation of Liquid Foods	6
RhinoCFD: CAD to CFD Powered by PHOENICS	10
News from CHAM and Its Agents	12